Accepted Manuscript

Practical preparation of UDP-apiose and its applications for studying apiosyltransferase

Tae Fujimori, Ryoko Matsuda, Mami Suzuki, Yuto Takenaka, Hiroyuki Kajiura, Yoichi Takeda, Takeshi Ishimizu

PII: S0008-6215(19)30056-4

DOI: https://doi.org/10.1016/j.carres.2019.03.011

Reference: CAR 7693

To appear in: *Carbohydrate Research*

Received Date: 29 January 2019

Revised Date: 19 March 2019

Accepted Date: 21 March 2019

Please cite this article as: T. Fujimori, R. Matsuda, M. Suzuki, Y. Takenaka, H. Kajiura, Y. Takeda, T. Ishimizu, Practical preparation of UDP-apiose and its applications for studying apiosyltransferase, *Carbohydrate Research* (2019), doi: https://doi.org/10.1016/j.carres.2019.03.011.

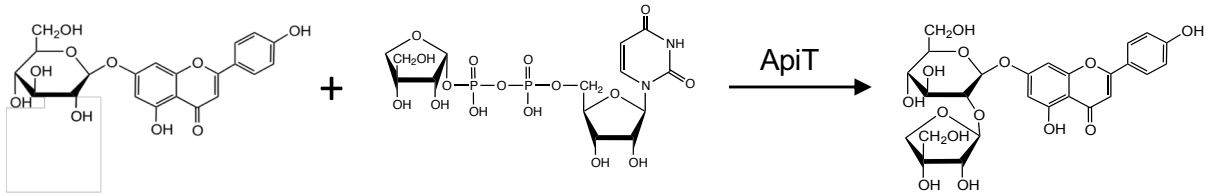

7-*O*-(β-Glucosyl)apigenin UDP-Apiose Apiin

Practical preparation of UDP-apiose and its applications for studying apiosyltransferase

Tae Fujimori[a,1], Ryoko Matsuda[a,1], Mami Suzuki[a], Yuto Takenaka[b], Hiroyuki Kajiura[a], Yoichi Takeda[a], Takeshi Ishimizu[a,b,*]

[a]College of Life Sciences, Ritsumeikan University, Kusatsu, Shiga 525-8577, Japan

[b]Ritsumeikan Global Innovation Research Organization, Ritsumeikan University, Kusatsu, Shiga 525-8577, Japan

*Corresponding author. Takeshi Ishimizu, College of Life Sciences, Ritsumeikan University, 1-1-1 Noji-Higashi, Kusatsu, Shiga, 5258577, Japan,

Tel.: +81-77-561-5973; Fax: +81-77-599-4358; E-mail: ishimizu@fc.ritsumei.ac.jp

[1]These authors contributed equally to this study.

Abbreviations: Api, apiose; AXS1, UDP-D-apiose/UDP-D-xylose synthase; GlcUA, glucuronic acid; PcApiT, *Petroselinum crispum* UDP-apiose: apigenin 7-*O*-β-D-glucoside apiosyltransferase; RG-II, rhamnogalacturonan II; Xyl, xylose

Abstract

UDP-apiose, a donor substrate of apiosyltransferases, is labile because of its intramolecular self-cyclization ability, resulting in the formation of apiofuranosyl-1,2-cyclic phosphate. Therefore, stabilization of UDP-apiose is indispensable for its availability and identifying and characterizing the apiosyltransferases involved in the biosynthesis of apiosylated sugar chains and glycosides. Here, we established a method for stabilizing UDP-apiose using bulky cations as counter ions. Bulky cations such as triethylamine effectively suppressed the degradation of UDP-apiose in solution. The half-life of UDP-apiose was increased to 48.1 ± 2.4 h at pH 6.0 and 25 °C using triethylamine as a counter cation. UDP-apiose coordinated with a counter cation enabled long-term storage under freezing conditions. UDP-apiose was utilized as a donor substrate for apigenin 7-*O*-β-D-glucoside apiosyltransferase to produce the apiosylated glycoside apiin. This apiosyltransferase assay will be useful for identifying genes encoding apiosyltransferases.

Key words: apiin, apiose, glycoside, glycosyltransferase, nucleotide sugar, UDP-apiose

1. Introduction

Apiose, a branched-chain pentose found in a wide variety of plants as a secondary metabolite [1], was originally discovered as a sugar component of the flavone glycoside apiin [2]. Apiin, apigenin-7-*O*-β-D-apiofuranosyl-(1→2)-β-D-glucopyranoside, is found in winter-hardy plants such as parsley and celery. Nearly 1,200 glycosides containing apiose residues have been identified [1]. Their aglycons include phenolics, terpens, terpenoids, cyanogenic glycosides, and alcohols. Although the role of apiosylation is unclear, some studies suggested that apiosylated compounds serve as cryoprotectants [3,4] and protect against oxidative stress [5]. Apiose residues are also found in apiogalacturonan and rhamnogalacturonan II (RG-II), which are pectic domains of the plant cell wall [6,7]. The apiose residue in RG-II provides scaffold for crosslinking with boron, resulting in the formation of a rigid cell wall by pectin dimerization [8,9]. Defects in the dimerization of RG-II resulting from a low-boron supply [10] or alterations in the structure of the side chain containing the apiosyl residue in RG-II [11,12] caused growth defects in Arabidopsis. Recently, apiose was detected in the acid hydrolysate of methanolic extracts from some bacteria species, although the structure of the apiosylated glycosides has not been determined [13,14].

UDP-α-D-apiose (UDP-Api) serves as an apiose donor for apiosylated compounds. This compound was first identified in parsley, as the acid hydrolysate of its sugar nucleotides fraction contained apiose [15]. UDP-Api was synthesized from UDP-glucuronic acid (UDP-GlcUA) by UDP-Api/UDP-xylose (UDP-Xyl) synthase (AXS) [16,17]. This enzyme catalyzes both decarboxylation of UDP-GlcUA and the subsequent re-arrangement of the carbon skeleton and ring contraction to form UDP-Api [18,19]. The synthesis of UDP-Api and UDP-Xyl occurs simultaneously, and these molecules cannot be interconverted [17]. Arabidopsis contains two *AXS* genes (*AXS1* and *AXS2*) and both are expressed in all plant tissues, suggesting that *AXS* genes have housekeeping function in Arabidopsis [17]. Knockdown plant of *NbAXS1* from *Nicotiana benthamiana* lacking the *AXS2* homolog resulted in severe defects in body development, abnormal

structure of the cell walls, and reduction of apiose, suggesting that an aberrant structure of RG-II causes severe phenotypical changes [20].

Apigenin 7-*O*-β-D-glucoside apiosyltransferase (EC 2.4.2.25) uses UDP-Api as a donor substrate to synthesize apiin [21]. Polygalacturonic acid apiosyltransferase, which is involved in the synthesis of RG-II or apiogalacturonan, is thought to use UDP-Api as a donor substrate, although their activities have not been detected so far. Biochemical characterization or gene identification of these apiosyltransferases has not progressed because UDP-Api is not commercially available. UDP-Api is quite unstable in solution and easily degraded to apiofuranosyl-1,2-cyclic phosphate and UMP [19, 22] by intramolecular nucleophilic substitution of phosphate with the hydroxyl group at the 2-position of apiose (Fig. 1A). The half-life of UDP-Api is 97.2 min at 25 °C and pH 8.0 [23], which is the optimum pH for the AXS reaction. Thus, UDP-Api synthesized enzymatically began to degrade spontaneously. At acidic pH, UDP-Api is degraded to α-D-apiose and UDP with a half-life of 4.67 min (pH 3.0 and 40 °C) [23]. Previous studies showed that apiosyltransferase activity [14,21] depends on UDP-Api instantaneously formed by AXS. The detection of such UDP-Api highly depends on real-time nuclear magnetic resonance (NMR) spectroscopy [24]. The NMR spectra observed for the AXS reaction mixture were derived from resulting compounds such as UMP, α-D-apio-furanosyl-1,2-cyclic phosphate, UDP-Xyl, and undegraded UDP-Api [24]. Therefore, establishing a method for stabilizing UDP-Api is important for understanding the dynamics of apiose both *in vivo* and *in vitro*.

In this study, we aimed to determine the effects of bulky counter cations on UDP-Api stability and half-life, to utilize it as a donor substrate for apiosyltransferases. Our method will improve the availability of apiose, which contributes not only to the characterization of apiosyltransferases and identification of their corresponding genes, but also to clarifying the roles of apiose residues in secondary metabolites or pectins.

2. Results and Discussion

2.1 Enzymatic synthesis of UDP-Api

UDP-Api is immediately degraded to UMP and apiofuranosyl-1,2-cyclic phosphate under alkaline conditions [23]. To prevent the degradation of UDP-Api, the effect of counter cations oriented to UDP-Api was investigated. The counter cations were predicted to bind the phosphate group of UDP-Api and escape from nucleophilic attack by the 2″-OH group on D-apiose to the adjacent phosphate group (Fig. 1A), resulting in degradation of UDP-Api.

AtAXS1, AXS from *Arabidopsis thaliana*, catalyzes the generation of UDP-Api and UDP-Xyl from UDP-GlcUA [17] (Fig. 1A). The recombinant AtAXS1 protein was reacted with UDP-GlcUA in 100 mM sodium phosphate buffer, pH 8.0. The reaction was stopped after incubation with the enzyme at 25 °C for 4 h and then further incubated for 4 h at the same temperature. This reaction mixture was analyzed by reverse phase HPLC. The reaction yielded only UDP-Xyl and UMP, which was a degradation product of UDP-Api (Fig. 1B, upper panel). This agreed with previous results showing that UDP-Api produced by AtAXS1 is immediately degraded in this solution [17,19]. When the reaction was performed in 100 mM triethylamine phosphate buffer, pH 8.0, an additional peak, which appeared to be UDP-Api, was detected (Fig. 1B, lower panel). The molecular mass of the compound in this peak was *m/z* 535.1, which agreed with the calculated mass of UDP-Api (*m/z* 535.0) (Fig. 1C). However, its molecular mass also corresponded to that of UDP-Xyl and thus this peak was further analyzed. UDP-Api degrades to UDP and Api under acidic conditions [23]. Incubation of this compound in 4 M trifluoroacetic acid at 95 °C for 30 min generated Api but not Xyl (Fig. 1D). The triethylamine salt of the compound dissolved in D_2O was analyzed by ^1H and 2D ^1H-^1H-COSY NMR spectroscopy (Fig. 1E and Fig. S1). The chemical shift and coupling constant values of the ribose and uracil rings agreed well with those of typical UDP-sugars [25]. The chemical shifts of H2″, H3″a, H3″b, H4″a, and H″4b of this compound (Table 1) were similar to those of free D-apiose [26]. COSY analysis of the compound (Fig. S1) revealed the connectivity from H1″ (5.61 ppm, apparent t, $J_{1'',2''}$ 4.7, $J_{1'',P}$ 5.4 Hz) to H2″ (3.91 ppm, dd, $J_{1'',2''}$ 4.7,

$J_{2'',P}$ 2.2 Hz). However, another connectivity pattern was not observed, indicating that no proton attached to the carbon atom between C2″ and C4″. The remaining peaks reflect the geminal protons of H3″a/b ($J_{3''a,3''b}$ 11.6 Hz) and H4”a/b ($J_{4''a,4''b}$ 10.3 Hz). The chemical shift of H1″ and the values of $J_{1'',P}$ and $J_{1'',2''}$ show the linkage between the anomeric apiose residue and phosphate of UDP. These assignments of UDP-Api do not contradict those of the tentatively generated UDP-Api in the reaction mixture containing UDP-Xyl, UMP, and α-D-apio-D-furanosyl-1,2-cyclic phosphate [24]. No signals derived from the degraded compounds of UDP-Api (UMP and α-D-apio-D-furanosyl-1,2-cyclic phosphate) were observed in these NMR spectra (Fig. 1E). These analyses demonstrate that this product was UDP-Api, showing that its triethylamine salt form was relatively stable in aqueous solution.

2.2 Effect of counter cations on the stability of UDP-Api

Triethylamine in the reaction mixture for enzymatic production of UDP-Api suppressed the degradation of UDP-Api, suggesting that a counter cation for UDP-Api may protect from a nucleophilic attack of 2″-OH to the phosphorus atom. Therefore, other various amines were investigated to determine their effects on the stability of UDP-Api. Triethylamine, a counter cation of phosphate buffer, was substituted for each amine, and UDP-Api was produced enzymatically under the conditions shown in Fig. 1B. The undegraded UDP-Api was quantified after a 4-h incubation at 25 °C in the presence of each counter cation (Fig. 2A). When sodium ion was used as a counter cation of phosphate buffer in the reaction mixture, only 6.2 ± 1.1% of UDP-Api remained. In contrast, a substantial amount of UDP-Api remained in the reaction mixture when bulky tertiary amines such as *N*-ethyldiisopropylamine (90.6 ± 2.1%), *N*,*N*-diethylcyclohexylamine (89.9 ± 2.9%), and triethylamine (82.7 ± 5.7%) were used as counter cations of phosphate buffer. Non-bulky amines such as ethylamine were less effective. Comparison of the effects among triethylamine (82.7 ± 5.7%), diethylamine (61.2 ± 1.5%), and ethylamine (10.2 ± 1.7%) showed that the bulkiness and/or hydrophobicity of the amines affected the stabilization of UDP-Api.

Triethylamine was selected as a counter cation of UDP-Api for further analysis because of its high efficiency for stabilizing UDP-Api and because of its convenience. The optimal concentration of triethylamine phosphate buffer, pH 8.0, in the reaction mixture for UDP-Api production was 100–200 mM. Triethylamine is empirically known to stabilize UDP-arabinofuranose [27],which is comparatively unstable because it has an axial 2'-OH similar to UDP-Api does. The preference of counter cations for stabilization of UDP-arabinofuranose would be similar to that for stabilization of UDP-Api.

To investigate the efficiencies of triethylamine on stabilizing UDP-Api at different buffer pHs, the time course of the remaining UDP-Api in each buffer at 25 °C was plotted (Fig. 2B). UDP-Api was declined logarithmically in the buffer investigated. These results were used to estimate the pseudo first-order rate constant for the degradation of UDP-Api and the half-life of UDP-Api (Table 2). The half-life of UDP-Api in 100 mM sodium phosphate buffer, pH 8.0, was 1.0 ± 0.1 h. This value is consistent with a previously reported value (1.6 h in 50 mM potassium phosphate buffer, pH 8.0) [23]. The substitution of sodium ion with triethylamine extended the half-life of UDP-Api to 22.5 ± 1.4 h. Lowering the pH to 6.0 extended the half-life to 30.5 ± 0.5 h. Simultaneous substitution of sodium ion with triethylamine and the lowering the pH to 6.0 prolonged the half-life of UDP-Api to 48.1 ± 2.4 h. The substitution of the sodium ion for triethylamine and changing the pH from 8.0 to pH 6.0, increased the half-life of UDP-Api. Both effects independently contributed to the stabilization of UDP-Api. Thus, the half-life of UDP-Api was more than 30-fold longer at pH 6.0 with triethylamine than that at 8.0 without triethylamine (Fig. 2B and Table 2). The enzymatic synthesis of UDP-Api could be carried out at pH 6.0: however, the AXS enzyme activity at pH 6.0 was around 40% of the activity at pH 8.0 under the presence of 100 mM triethylamine phosphate buffer. The maximum final yield of UDP-Api was observed when the enzymatic synthesis was carried out at pH 8.0 and the product was stored at pH 6.0 in the presence of triethylamine. Therefore, the enzymatic synthesis of UDP-Api was carried out at pH 8.0 in the presence of triethylamine in this study.

The stabilization of UDP-Api was temperature-dependent (Fig. 2C). In the sodium phosphate buffer (pH 8.0), nearly all UDP-Api was degraded at 25 °C after a 4-h incubation. In contrast, UDP-Api was relatively stable in the triethylamine phosphate buffer (pH 6.0) at less than 25 °C. Even when triethylamine was used as a counter cation, nearly all UDP-Api was degraded at 50 °C over 4 h of incubation. Storage at low temperatures led to the stabilization of UDP-Api and the compound could be stored at -80 °C for at least 2 months without degradation. This is a practical storage condition for UDP-Api.

2.3 Detection of apiosyltransferase activity

The presence of apiosylated sugar chains and glycosides in plants suggests that some apiosyltransferases are encoded by plant genomes. The amount of UDP-Api prepared in this study was sufficient for use as a donor substrate of apiosyltransferase. The activity of parsley *Petroselinum crispum* apigenin 7-*O*-β-D-glucoside apiosyltransferase (PcApiT), which catalyzes the formation of apiin, can be detected using transiently generated UDP-Api [21]. This PcApiT activity was investigated using the UDP-Api prepared in this study. The crude extract of parsley young leaves [28] was used as an enzyme source. The reaction mixture containing 50 μM apigenin 7-*O*-β-D-glucoside, 1 mM UDP-Api, and crude enzyme solution was incubated at 25 °C and pH 7.0 [29]. The 2-h incubation of the reaction mixture generated new compounds observed on a revered-phase chromatogram (Fig 3A). The elution time corresponded to that of authentic apiin. The molecular mass of this compound $[M-H]^-$ was m/z 563.7 (Fig. 3B), which agreed with its calculated molecular mass. These results show that a bulky counter cation for UDP-Api had no fatal inhibitory effect on apiosyltransferase activity. The K_m and apparent V_{max} values for apigenin 7-*O*-β-D-glucoside were 118 ± 6 μM and 3.28 ± 0.81 nmol·min^{-1}·mg^{-1} protein, respectively (Fig. 3C). This K_m value is equivalent to those reported previously [29]. The K_m and apparent V_{max} values for UDP-Api were 920 ± 230 μM and 7.5 ± 1.1 nmol·min^{-1}·mg^{-1} protein, respectively (Fig. 3D).

More than 20 nucleotide sugars have been identified in plant cells and are required for the biosynthesis of various glycan compounds including secondary metabolites and plant cell wall polysaccharides [30]. Each nucleotide sugar is utilized as a donor substrate for specific glycosyltransferases. However, numerous sugar nucleotides are not commercially available, partially because of the instability of some nucleotide sugars. The method for stabilizing nucleotide sugars with counter cations presented in this study can be applied to stabilize and isolate other unstable sugar nucleotides such as UDP-arabinofuranose [27,31] and CMP-Kdo [32], which are critical compounds for the biosynthesis of plant cell wall polysaccharides.

Developing an assay for evaluating apiin-synthetic apiosyltransferase activity will be useful for further biochemical characterization of this enzyme. Additionally, UDP-Api is used for biochemical assays involving pectin rhamnogalacturonan II-synthetic apiosyltransferase. These biochemical assays can be used to identify genes encoding apiosyltransferases based on the progress of plant genome science.

4. Materials and Methods

4.1 Materials

cDNA (pda01652) encoding *AtAXS1* was obtained from the RIKEN BioResource Center (Ibaraki, Japan) [33]. β-NAD^+ and UDP-GlcUA were purchased from Sigma (St. Louis, MO, USA) and Yamasa (Tokyo, Japan), respectively. *N*,*N*-Dimethylcyclohexylamine, *N*,*N*-diethylcyclohexylamine, diisopropylamine, *N*,*N*-diisopropylethylamine, trimethylamine, ethylamine, diethylamine, triethylamine, hexamethylenediamine, bis(2-aminoethyl)amine, and isophoronediamine were purchased from Fujifilm Wako Pure Chemical Corporation (Osaka, Japan). Apigenin 7-*O*-β-D-glucoside and apiin were obtained from Ark Pharm (Arlington Heights, IL, USA). UDP-Xyl was synthesized as described previously [25].

4.2 Enzymatic synthesis of UDP-Api

The recombinant AtAXS1 protein was prepared as described previously [17]. The enzymatic synthesis of UDP-Api was carried out in a reaction mixture comprising 100 mM triethylamine phosphate buffer, pH 8.0, 50 mM UDP-GlcUA, 0.5 mM NAD^+ and 10 μg/μL of the purified protein. The reaction mixtures were incubated at 25°C for 4 h and the reaction was terminated by adding phenol/chloroform/isoamyl alcohol (25:24:1, v/v/v), followed by vigorous shaking. The water phase containing the reaction products was obtained by centrifugation (22,000 ×*g* at 4°C for 5 min) and subjected to analysis.

The reaction products were separated and monitored by a reversed phase (RP)-HPLC equipped with a UV detector. RP-HPLC was performed using an Inertsil ODS-3 column (4.6 × 250 mm; GL Sciences, Tokyo, Japan) with an L-6200 intelligent pump and L-4000 UV detector (Hitachi High-Technologies, Tokyo, Japan) at a flow rate of 1.2 mL/min. The mobile phase was composed of 100 mM *N*,*N*-dimethylcyclohexylamine phosphate buffer, pH 6.5. The eluted fractions were monitored by measuring the absorbance at 262 nm.

4.3 Effect of counter cations on the stability of UDP-Api

UDP-Api generated by enzymatic reaction was incubated at 25°C for a further 4 h in the presence of various amine compounds. The undegraded UDP-Api was quantified by RP-HPLC. The reported values are the averages of three independent experiments with standard errors. To determine the half-life of UDP-Api in the presence of counter cations, the AtAXS1 reaction was carried out and stopped as described above. Next, the reaction mixture was incubated at 25°C. The residual UDP-Api was quantified from the RP-HPLC peak areas of UDP-Api at each time point.

4.4 Structural analysis of UDP-Api

The UDP-Api produced enzymatically was purified and collected by RP-HPLC. The molecular mass of UDP-Api was determined by flow injection into an LCMS-2020 mass spectrometer equipped with a LC-20AD HPLC pump (Shimadzu, Kyoto, Japan) at a flow rate of 0.2 mL/min of 50% acetonitrile.

The lyophilized UDP-Api was dissolved in D_2O (D, 99.9%), freeze dried, and then dissolved in D_2O again for NMR analysis. ^{1}H-NMR spectra (1D, 2D-COSY) were recorded with an ECA-600HR NMR spectrometer (JEOL, Tokyo, Japan) at ambient temperature. Acid hydrolysis of UDP-Api was conducted in 4 M trifluoroacetic acid at 90°C for 30 min. The acid hydrolysate was separated using an UnisonUK-Amino column (4.6 × 250 mm; Imtakt, Kyoto, Japan) and detected with an ELSD-LTII evaporative light scattering detector (Shimadzu). The column was equilibrated with 95% acetonitrile in distilled water at a flow rate of 1.0 mL/min at 45°C. Linear gradient elution was performed by decreasing the concentration of acetonitrile to 70% over 25 min.

4.5 Apiosyltransferase assay

The young leaves (1 g) of parsley (*Apium petroselinum* L.) were pulverized with a pestle on ice in 1 mL of extraction buffer containing 150 mM Tris-HCl buffer, pH 7.0, 30 mM ascorbic acid, and 0.1% 2-mercaptoethanol. The homogenate was centrifuged at 20,000 ×*g* for 10 min at 4°C. The enzyme in this supernatant was concentrated using Amicon Ultra-15 centrifugal filter units (Millipore, Billerica, MA, USA) and used as the crude enzyme solution. The apigenin 7-*O*-β-D-glucoside apiosyltransferase assay was conducted with 50 μM apigenin 7-*O*-β-D-glucoside, 1 mM UDP-Api, and 8.0 μg/μL of a crude enzyme in 100 mM Tris-HCl buffer, pH 7.0, containing 50 mM NaCl for 2 h at 23°C. The reaction products were separated by RP-HPLC using an Inertsil ODS-3 column at a flow rate of 1.0 mL/min with an isocratic flow of 20% acetonitrile containing 0.1% trifluoroacetic acid for initial 5 min, followed by a linear gradient from 20 to 40% acetonitrile for 20 min. The eluates were monitored by absorbance at 330 nm. The K_m and V_{max} values of the enzyme were determined by assaying with various concentrations of apigenin 7-*O*-β-D-glucoside (50–200 μM) or UDP-Api (125–1,000 μM). The mean values of triplicate experimentals with standard deviation were plotted on a Michaelis-Menten plot, and the kinetic parameters were calculated. Kinetic data were calculated by non-linear regression analysis using Prism version 8 (GraphPad Software, San Diego, CA).

Author contribution statement

TI designed and supervised the research. MS initiated the research and TF and RM performed most of the experiments. YT, HK, YT, and TI analyzed the data. TF, YT, HK, YT, and TI wrote the manuscript.

Conflicts of interest

The authors declare that they have no conflicts of interest.

Funding: This work was supported by Grants-in-Aid for Scientific Research (Grant Numbers JP15K07016 and JP18H05495) from the Ministry of Education, Culture, Sports, Science and Technology of Japan. The study was also supported by the Program for the Third-Phase R-GIRO Research from the Ritsumeikan Global Innovation Research Organization, Ritsumeikan University.

References

[1] M. Pičmanová, B.L. Møller, Apiose: one of nature's witty games, Glycobiology 26 (2016) 430–442. https://doi.org/10.1093/glycob/cww012.

[2] E. Vongerichten, Uber das Apiin und Apiose, Liebigs Ann. Chem. 318 (1901) 121–136. https://doi.org/10.1002/jlac.19013180106.

[3] R.R. Watson, N.S. Orenstein, Chemistry and biochemistry of apiose, Adv. Carbohydr. Chem. Biochem. 31 (1975) 135–184. https://doi.org/10.1016/S0065-2318(08)60296-6

[4] E. Beck, H. Hopf, Branched-chain sugars and sugar alcohols, Methods Plant Biochem. 2 (1990) 235–289. https://doi.org/10.1016/B978-0-12-461012-5.50013-6.

[5] H. Eckey-Kaltenbach, W. Heller, J. Sonnenbichler, I. Zetl, W. Schäfer, D. Ernst, H. Sandermann, Oxidative stress and plant secondary metabolism: 6"-*O*-malonylapiin in parsley, Phytochemistry 34 (1993) 687–691. https://doi.org/10.1016/0031-9422(93)85340-W.

[6] D.A. Hart, P.K. Kindel, Isolation and partial characterization of apiogalacturonans from the cell wall of *Lemna minor*, Biochem. J. 116 (1970) 569–579. https://doi.org/10.1042/bj1160569.

[7] A.G. Darvill, M. McNeil, P. Albersheim, Structure of plant cell walls: VIII. A new pectic polysaccharide, Plant Physiol. 62 (1978) 418–422. https://doi.org/10.1104/pp.62.3.418.

[8] M. Kobayashi, T. Matoh, J. Azuma, Two chains of rhamnogalacturonan II are cross-linked by borate-diol ester bonds in higher plant cell walls, Plant Physiol. 110 (1996) 1017–1020. https://doi.org/10.1104/pp.110.3.1017.

[9] M.A. O'Neill, D. Warrenfeltz, K. Kates, P. Pellerin, T. Doco, A.G. Darvill, P. Albersheim, Rhamnogalacturonan-II, a pectic polysaccharide in the walls of growing plant cell, forms a dimer that is covalently cross-linked by a borate ester. *In vitro* conditions for the formation and hydrolysis of the dimer, J. Biol. Chem. 271 (1996) 22923–22930. https://doi.org/10.1074/jbc271.37.22923.

[10] K. Miwa, S. Wakuta, S. Takada, K. Ide, J. Takano, S. Naito, H. Omori, T. Matsunaga, T. Fujiwara, Roles of BOR2, a boron exporter, in cross linking of rhamnogalacturonan II and root

elongation under boron limitation in Arabidopsis, Plant Physiol. 163 (2013) 1699–1709. https://doi.org/10.1104/pp.113.225995.

[11] M.A. O'Neill, S. Eberhard, P. Albersheim, A.G. Darvill, Requirement of borate cross-linking of cell wall rhamnogalacturonan II for Arabidopsis growth, Science 294 (2001) 846–849. https://doi.org/10.1126/science.1062319.

[12] J. Sechet, S. Htwe, B. Urbanowicz, A. Agyeman, W. Feng, T. Ishikawa, M. Colomes, K.S. Kumar, M. Kawai-Yamada, J.R. Dinneny, M.A. O'Neill, J.C. Mortimer, Suppressing Arabidopsis GGLT1 affects growth by reducing the L-galactose content and borate cross-linking of rhamnogalacturonan II, Plant J. 96 (2018) 1036–1050. https://doi.org/10.1111/tpj.14088.

[13] J.A. Smith, M. Bar-Peled, Synthesis of UDP-apiose in bacteria: The marine phototroph *Geminicoccus roseus* and the plant pathogen *Xanthomonas pisi*, PLoS One 12 (2017) e0184953. https://doi.org/10.1371/journal.pone.0184953.

[14] J.A. Smith, M. Bar-Peled, Identification of an apiosyltransferase in the plant pathogen *Xanthomonas pisi*, PLoS One 13 (2018) e0206187. https://doi.org/10.1371/journal.pone.0206187.

[15] H. Sandermann, H. Grisebach, Occurrence of UDP-apiose in parsley (*Apium petroselium* L.), Biochim. Biophys. Acta 156 (1968) 435–436. https://doi.org/10.1016/0304-4165(68)90282-1.

[16] H. Sandermann, G.T. Tisue, H. Grisebach, Biosynthesis of D-apiose: IV. Formation of UDP-apiose from UDP-D-glucuronic acid in cell-free extracts of parsley (*Apium petroselinum* L.) and *Lemna minor*, Biochim. Biophys. Acta 165 (1968) 550–552. https://doi.org/10.1016/0304-4165(68)90239-0.

[17] M. Mølhøj, R. Verma, W.D. Reiter, The biosynthesis of the branched-chain sugar D-apiose in plants: functional cloning and characterization of a UDP-D-apiose/UDP-D-xylose synthase from Arabidopsis, Plant J. 35 (2003) 693–703. https://doi.org/10.1046/j.1365-313X.2003.01841.x.

[18] C. Gebb, D. Baron, H. Grisebach, Spectroscopic evidence for the formation of a 4-keto intermediate in the UDP-apiose/UDP-xylose synthase reaction, Eur. J. Biochem. 54 (1975) 493–498. https://doi.org/10.1111/j.1432-1033.1975.tb04161.x.

[19] T. Eixelsberger, D. Horvat, A. Gutmann, H. Weber, B. Nidetzky, Isotope probing of the UDP-apiose/UDP-xylose synthase reaction: evidence of a mechanism via a coupled oxidation and aldol cleavage, Angew. Chem. Int. Ed. 56 (2017) 2503–2507. https://doi.org/10.1002/anie.201609288.

[20] J.W. Ahn, R. Verma, M. Kim, J.Y. Lee, Y.K. Kim, J.W. Bang, W.D. Reiter, H.S. Pai, Depletion of UDP-D-apiose/UDP-D-xylose synthases results in rhamnogalacturonan-II deficiency, cell wall thickening, and cell death in higher plants, J. Biol. Chem. 281 (2006) 13708–13716. https://doi.org/10.1074/jbc.M512403200.

[21] R. Ortmann, H. Sandermann, H. Grisebach, Transfer of apiose from UDP-apiose to 7-*O*-(β-D-glucosyl)-apigenin and 7-*O*-(β-D-glucosyl)-chrysoeriol with an enzyme preparation from parsley, FEBS Lett. 7 (1970) 164–166. https://doi.org/10.1016/0014-5793(70)80146-6.

[22] D.L. Gustine, P.K. Kindel, Biosynthesis of D-apiose in a cell-free system from *Lemna minor* L., J. Biol. Chem. 244 (1969) 1382–1385.

[23] P.K. Kindel, R.R. Watson, Synthesis, characterization and properties of uridine 5'-(α-D-apio-D-furanosyl pyrophosphate), Biochem. J. 133 (1973) 227–241. https://doi.org/10.1042/bj1330227.

[24] P. Guyett, J. Glushka, X. Gu, M. Bar-Peled, Real-time NMR monitoring of intermediates and labile products of the bifunctional enzyme UDP-apiose/UDP-xylose synthase, Carbohydr. Res. 344 (2009) 1072–1078. https://doi.org/10.1016/j.carres.2009.03.026.

[25] T. Ishimizu, T. Uchida, K. Sano, S. Hase, Chemical synthesis of uridine 5'-diphospho-α-xylophyranose, Tetrahedron Asymm. 16 (2005) 309–311. https://doi.org/10.1016/j.tetasy.2004.11.073.

[26] J.R. Snyder, A.S. Serianni, DL-Apiose substituted with stable isotopes: synthesis, N.M.R.-spectral analysis, and furanose anomerization, Carbohydr. Res. 166 (1987) 85–99. https://doi.org/10.1016/0008-6215(87)80046-0.

[27] Q. Zhang, N.J. Shirley, R.A. Burton, J. Lahnstein, M. Hrmova, G.B. Fincher, The genetics, transcriptional profiles, and catalytic properties of UDP-α-D-xylose 4-epimerases from barley, Plant Physiol. 153 (2010), 555–568. https://doi.org/10.1104/pp.110.157644

[28] K. Hahlbrock, A. Sutter, E. Wellmann, R. Ortmann, H. Grisebach, Relationship between organ development and activity of enzymes involved in flavone glycoside biosynthesis in young parsley plants, Phytochemistry 10 (1971) 109–116. https://doi.org/10.1016/ S0031-9422(00)90257-7.

[29] R. Ortmann, A. Sutter, H. Grisebach, Purification and properties of UDPapiose: 7-*O*-(β-D-glucosyl)-flavone apiosyltransferase from cell suspension cultures of parsley, Biochim. Biophys. Acta 289 (1972) 293–302. https://doi.org/10.1016/0005-2744(72)90080-0.

[30] M. Bar-Peled, M.A. O'Neill, Plant nucleotide sugar formation, interconversion, and salvage by sugar recycling, Annu. Rev. Plant Biol. 62 (2011) 172–155. https://doi.org/10.1146/annurev-arplant-042110-103918.

[31] T. Konishi, T. Takeda, Y. Miyazaki, M. Ohnishi-Kameyama, T. Hayashi, M.A. O'Neill, T. Ishii, A plant mutase that interconverts UDP-arabinofuranose and UDP-arabinopyranose, Glycobiology 17 (2007) 345–354. https://doi.org/10.1093/glycob/cwl081.

[32] C.H. Lin, B.W. Murray, I.R. Ollmann, C.H.Wong, Why is CMP-ketodeoxyoctonate highly unstable? Biochemistry 36 (1997) 780–785. https://doi.org/10.1021/bi962055c.

[33] M. Seki, M. Narusaka, A. Kamiya, J. Ishida, M. Satou, T. Sakurai, M. Nakajima, A. Enju, K. Akiyama, Y. Oono, M. Muramatsu, Y. Hayashizaki, J. Kawai, P. Carninci, M. Itoh, Y. Ishii, T. Arakawa, K. Shibata, A. Shinagawa, K. Shinozaki, Functional annotation of a full-length Arabidopsis cDNA collection, Science 296 (2002) 141–145. https://doi.org/10.1126/science.1071006.

Figure legends

Fig. 1. Enzymatic synthesis of UDP-Api using triethylamine as a counter cation. A) The scheme of enzymatical preparation of UDP-Api and degradation of UDP-Api in solution. AtAXS1 catalyzes conversion from UDP-GlcUA to UDP-Xyl and UDP-Api. UDP-Api is degraded to apiofuranosyl-1,2-cyclic phosphate and UMP. B) Analysis of the reaction products of AtAXS1 in the presence of triethylamine. UDP-GlcUA was reacted with AtAXS1 in the absence (upper panel) and presence (lower panel) of triethylamine as a counter cation at 25 °C for 4 h, stopped, and then incubated at the same temperature for an additional 4 h. The products were separated by reversed phase HPLC. The peaks were identified by comparison with the elution time (black wedges) of authentic UMP and UDP-Xyl. UDP-Api was identified by the following analyses. C) Mass spectrum of UDP-Api determined by ESI-IT MS in negative ion mode. The calculated molecular mass of $[M-H]^-$ ions of UDP-pentose was 535.1. D) Monosaccharide analysis of the acid hydrolysate of UDP-Api. The acid hydrolysates of UDP-Xyl (upper panel) and UDP-Api (lower panel) were analyzed with an UnisonUK-Amino column and detected with an evaporative light scattering detector. The peaks were identified by comparison with the elution time (black wedges) of authentic Xyl and Api. E) ^{1}H-NMR spectrum of UDP-Api. Each peak was assigned from 2D-COSY spectrum of UDP-Api. The chemical shifts of protons are shown in Table 1.

Fig. 2 Effect of counter cations on UDP-Api stability. A) Percentage of undegraded UDP-Api in the presence of various amine compounds. The UDP-Api was incubated in 100 mM phosphate buffer, pH 8.0, containing each amine compound as counter cation at 25°C for 4 h. The values are presented as the average of three independent experiments with standard errors. B) Time-course of degradation of UDP-Api in various buffers. The percentage of undegraded UDP-Api in the buffers at 25 °C was plotted against time. The buffers used were 100 mM sodium phosphate buffer, pH 8.0 (closed diamond), 100 mM sodium phosphate buffer, pH 6.0 (closed circle),100 mM triethylamine phosphate buffer, pH 8.0 (open diamond), and 100 mM triethylamine phosphate buffer, pH 6.0

(open circle). The mean values with standard errors for three independent experiments are plotted. The pseudo-first order rate constants for the degradation of UDP-APi and half-lives of UDP-Api in the buffers are shown in Table 2. C) Thermal stability of UDP-Api. The percentage of undegraded UDP-Api in the buffers at various temperature for 4 h were plotted. The buffers used were 100 mM sodium phosphate buffer, pH 8.0 (closed diamond), 100 mM sodium phosphate buffer, pH 6.0 (closed circle),100 mM triethylamine phosphate buffer, pH 8.0 (open diamond), and 100 mM triethylamine phosphate buffer, pH 6.0 (open circle). The mean values with standard errors for three independent experiments are plotted.

Fig. 3 Apiin-synthetic apiosyltransferase activity. A) The activity of apigenin 7-*O*-β-D-glucoside apiosyltransferase from parsley, *Petroselinum crispum* (PcApiT). The crude enzyme containing PcApiT was reacted with UDP-Api and apigenin 7-*O*-β-D-glucoside used as a donor and acceptor substrate, respectively, at 23°C for 0 h (upper panel) and 2 h (lower panel). The peaks were identified by comparison with the elution time of the authentic apigenin 7-*O*-β-D-glucoside (white wedge) and apiin (black wedge). B) The molecular mass of the PcApiT product determined by ESI-IT MS in positive ion mode. The calculated molecular mass of $[M-H]^-$ ions of apiin is 563.7. C) Michaelis-Menten kinetics of PcApiT on apigenin 7-*O*-β-D-glucoside. D) Michaelis-Menten kinetics of PcApiT on UDP-Api. The mean values of triplicate experimentals with standard deviation were plotted. The solid lines represent the theoretical non-linear regression fits of the data.

Supplementary data

Fig. S1. The 2D ^{1}H-^{1}H COSY NMR analysis of UDP-Api. Relevant cross-peaks are labeled as in Fig. 1E. Proton chemical shifts are reported in Table 1.

Table 1. ^{1}H signal assignment of UDP-Api. The value for proton chemical shifts of the UDP-Api triethylamine salt in D_2O at 25°C are shown.

Apiose		H1”	H2”	H3”a/3”b	H4”a/4”b	
	δ (ppm)	5.61	3.91	3.50	4.00	
Ribose		H1’	H2’	H3’	H4’	H5’a/5’b
	δ (ppm)	5.88	4.27	4.27	4.16	4.10
Uracil		H5	H6			
	δ (ppm)	5.87	7.86			

Chemical shifts are in ppm relative to internal H_2O signal set at 4.72 ppm.

Table 2. Pseudo first-order rate constant for the degradation of UDP-Api and half-life of UDP-Api in the various buffers.

Buffer	Pseudo first-order rate constant (h^{-1})	Half-life (h)
100 mM Sodium phosphate buffer, pH 8.0	0.29 ± 0.03	1.0 ± 0.1
100 mM Triethylamine phosphate buffer, pH 8.0	0.013 ± 0.001	22.5 ± 1.4
100 mM Sodium phosphate buffer, pH 6.0	0.0099 ± 0.0001	30.5 ± 0.5
100 mM Triethylamine phosphate buffer, pH 6.0	0.0063 ± 0.0003	48.1 ± 2.4

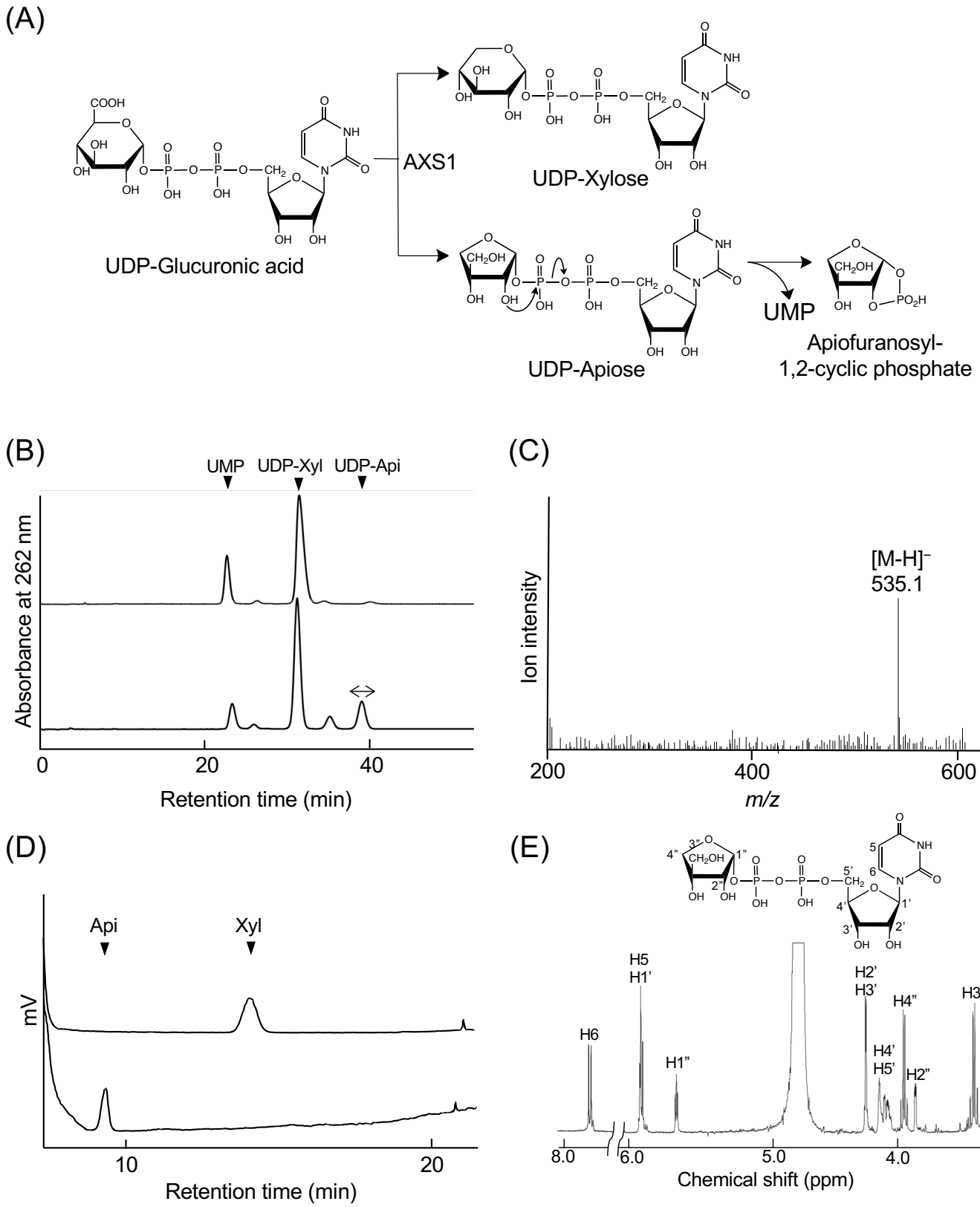
(A)
AXS1
UDP-Glucuronic acid
UDP-Xylose
UDP-Apiose
UMP
Apiofuranosyl-
1,2-cyclic phosphate
(B)
UMP
UDP-Xyl
UDP-Api
Absorbance at 262 nm
0
20
40
Retention time (min)
(C)
Ion intensity
[M-H]⁻
535.1
200
400
600
m/z
(D)
Api
Xyl
mV
10
20
Retention time (min)
(E)
H6
H5
H1'
H1"
H2'
H3'
H4"
H4'
H5'
H2"
H3"
8.0
6.0
5.0
4.0
Chemical shift (ppm)

Fig. 1

(A)

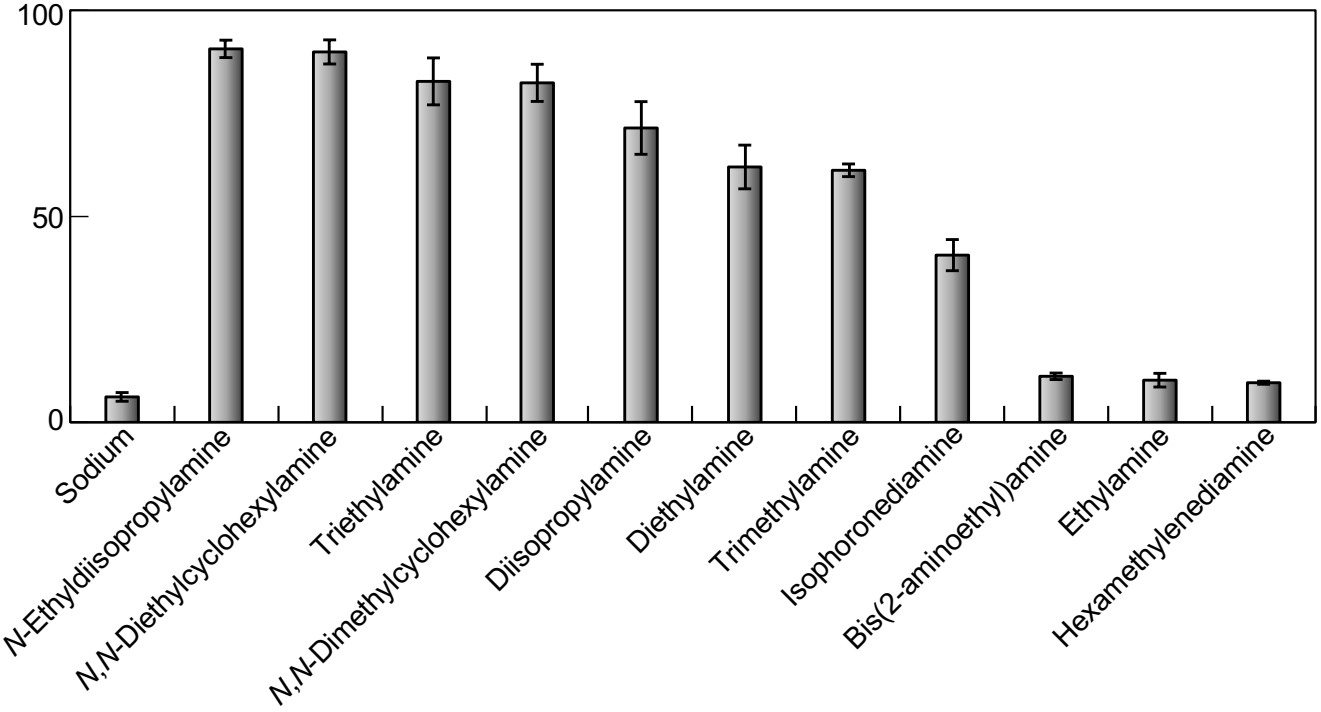
100
50
0
Sodium
N-Ethyldiisopropylamine
N,N-Diethylcyclohexylamine
Triethylamine
N,N-Dimethylcyclohexylamine
Diisopropylamine
Diethylamine
Trimethylamine
Isophoronediamine
Bis(2-aminoethyl)amine
Ethylamine
Hexamethylenediamine

(B)

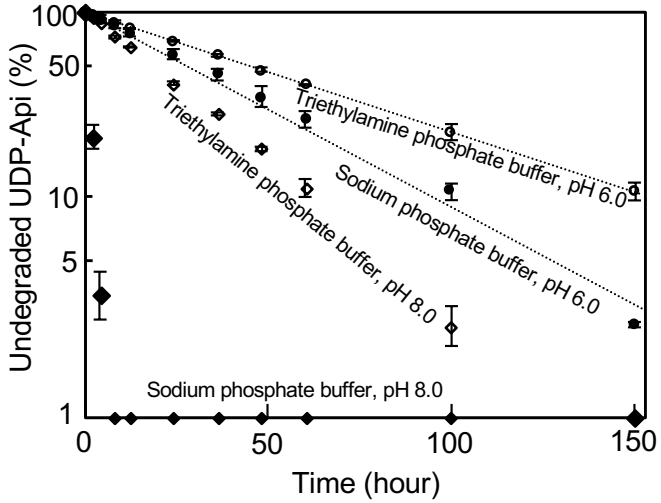
Undegraded UDP-Api (%)
100
50
10
5
1
0
50
100
150
Time (hour)
Triethylamine phosphate buffer, pH 6.0
Triethylamine phosphate buffer, pH 8.0
Sodium phosphate buffer, pH 6.0
Sodium phosphate buffer, pH 8.0

(C)

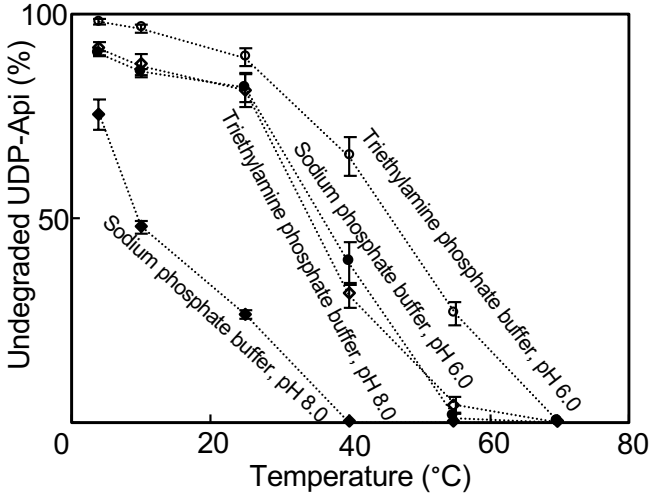
Undegraded UDP-Api (%)
100
50
0
20
40
60
80
Temperature (°C)
Triethylamine phosphate buffer, pH 6.0
Triethylamine phosphate buffer, pH 8.0
Sodium phosphate buffer, pH 6.0
Sodium phosphate buffer, pH 8.0

Fig. 2

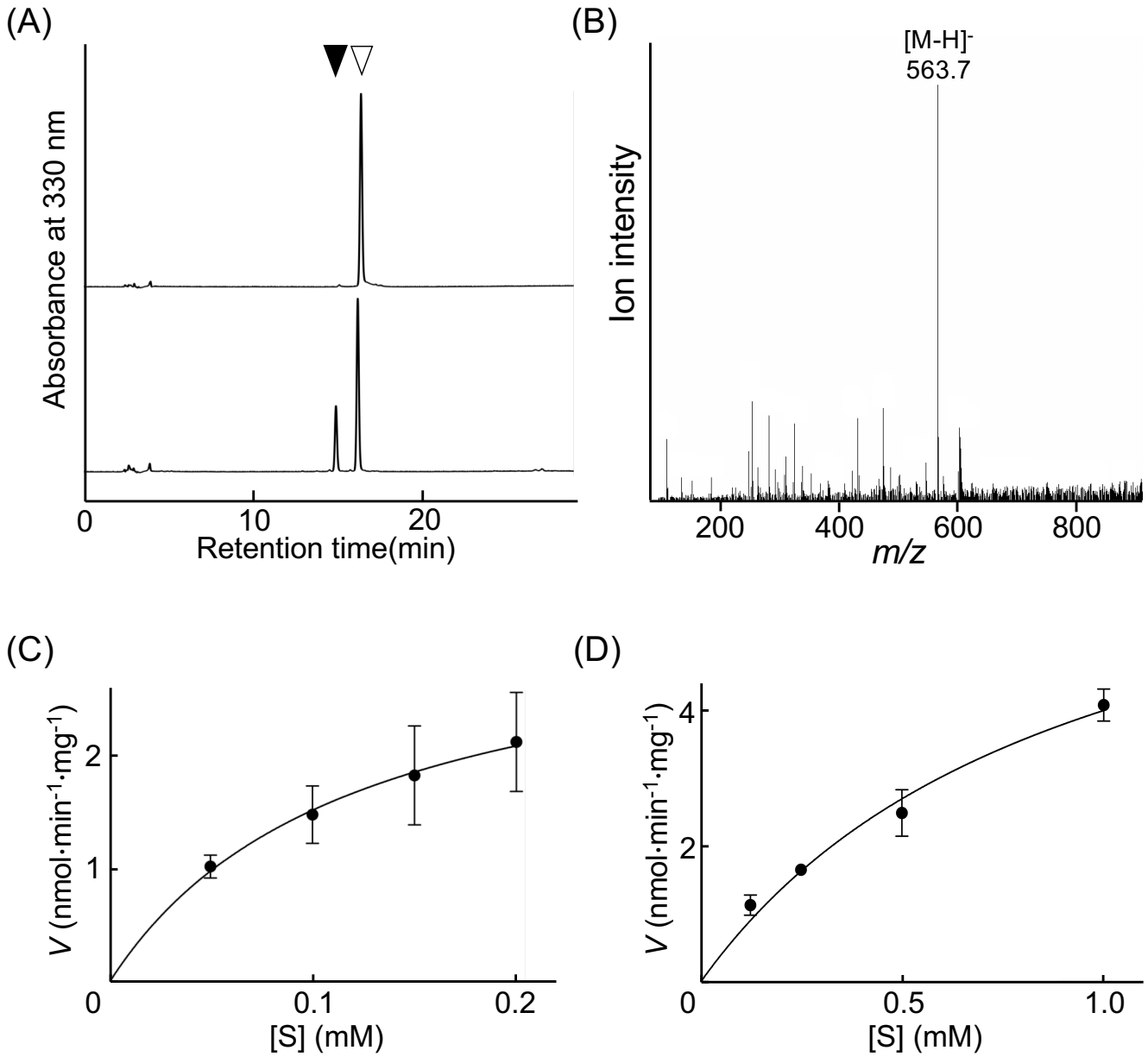
(A)
Absorbance at 330 nm
0
10
20
Retention time(min)
(B)
[M-H]-
563.7
Ion intensity
200
400
600
800
m/z
(C)
V (nmol·min-1·mg-1)
0
1
2
0
0.1
0.2
[S] (mM)
(D)
V (nmol·min-1·mg-1)
0
2
4
0
0.5
1.0
[S] (mM)

Fig. 3

Highlights

• UDP-apiose was stabilized in the presence of triethylamine.

• The half-life of UDP-apiose was increased to 48.1 h in solution.

• Apiin-producing apiosyltransferase activity was detected using UDP-apiose.